Macromolecules, 2015, 48 (8), pp 2561–2569

DOI: 10.1021/acs.macromol.5b00275

http://pubs.acs.org/doi/abs/10.1021/acs.macromol.5b00275

Determination of nucleus density in semicrystalline polymers from non-isothermal crystallization curves

Alfréd Menyhárd[1,2*], *Márton Bredács*[2], *Gergely Simon*[2], *Zsuzsanna Horváth*[1,2]

[1]Laboratory of Plastics and Rubber Technology, Department of Physical Chemistry and Materials Science, Budapest University of Technology and Economics, H-1111 Budapest, Műegyetem rakpart 3. H/1, Hungary

[2]Institute of Materials Science and Environmental Chemistry, Research Center for Natural Sciences, Hungarian Academy of Sciences, H-1117 Budapest, Magyar tudósok körútja 2., Hungary

[*] To whom correspondence should be addressed: Alfréd Menyhárd (amenyhard@mail.bme.hu)

ABSTRACT

The present study introduces a new calculation method for obtaining nucleus density formed during non-isothermal crystallization of semicrystalline polymers. Isotactic polypropylene homopolymer (iPP) was used as a semicrystalline model polymer and its crystalline structure was modified using highly efficient nucleating agents or different cooling rates in order to manipulate nucleus density (*N*) within a wide range. The melting and crystallization characteristics were studied by calorimetry (DSC) and the nucleus density was calculated from the crystallization curves recorded under non-isothermal conditions at constant cooling rate. The nucleus density was correlated to the optical property, in fact to the haze index of injection molded plaques in order to qualify the calculated values of *N*. It was found that *N* increases more orders of magnitude in nucleated samples and correlates strongly to the optical properties. These observations are according to our expectations and indicate clearly the reliability of the proposed calculation approach.

Keywords: nucleus density, crystallization kinetics, polypropylene, non-isothermal crystallization, optical properties

INTRODUCTION

Optical properties of semi-crystalline polymers are in the focus of the recent development in the polymer industry. The demand for optically transparent packaging materials increased dramatically in the last decades. Optically transparent engineering polymers like PMMA, PVC and PS were used in this area, but the cost of these materials made the packaging quite expensive. Consequently,

isotactic polypropylene (iPP) due to its exceptionally advantageous prize-performance ratio could be a potentially good candidate in packaging industry. On the contrary to the above-mentioned amorphous polymers iPP is a semicrystalline polymer [1]. The crystalline phase in iPP consist of different supermolecular entities formed from the arrangement of chain folded fibrillar or lamellar primer crystallites. Light scatters on these units, which makes iPP opaque, consequently reduces its applicability as transparent packaging material [2]. The optical properties of transparent products is characterized by haze, which is the total flux of light scattered within the angular range between 2.5 and 90° and normalized to the total transmitted flux [3]. The modification of crystalline structure by efficient nucleating agents is the most widely applied technique for improvement of optical and/or mechanical properties of iPP [1, 4-7]. Recently, sorbitol derivatives are used for clarifying iPP thus these additives are also called as clarifiers [8-18]. The former results indicated that nucleus density increases steeply in the presence of nucleating agents or clarifiers and consequently the size of supermolecular unit decreases considerably [19]. The presence of smaller supermolecular units changes the nature of light scattering in the visible range and results in smaller haze in the product [3].

Earlier studies revealed that nucleus density is a key parameter in understanding of optical properties in crystalline polymers [3, 19]. Several attempts were carried out for the reliable determination of nucleus density during crystallization [20-23]. The easiest technique is the estimation of nucleus density by optical or any other microscopic technique [24, 25]. Usually samples are crystallized in a microscope under isothermal conditions and the number of the nuclei formed can be counted directly in a small volume of the sample. The final N is given in one cubic meter. This method is effective and easy, but notoriously imprecise. Moreover, it works only in the temperature range wherein the number of spherulites can be counted. At low temperatures the number of

spherulites is too large and can not be counted reliably and at high temperatures the nucleus density is too small to obtain reliable result using this microscopic technique.

An other possibility is the determination of nucleus density from calorimetric crystallization curve, which can be described by kinetic equations. The most frequently applied kinetic concept for evaluation of crystallization process is the Avrami-Kolmogoroff-Evans equation (AKE) [26, 27], which is known as Avrami model.

$$E(t) = kt^n = \ln(2)\left(\frac{t}{t_{1/2}}\right)^n \tag{1}$$

$E(t)$ is the expected volume of crystalline phase, k is the overall rate constant of crystallization, t is the time and n is the Avrami exponent. Equation 1 can be applied for both thermal and athermal nucleation (see in Equation 2). The major difference in the nucleation mechanisms is that the number of nuclei is changing in thermal and remains constant in athermal nucleation under isothermal conditions.

$$E(t) = \begin{Bmatrix} N\nu(\theta,t) \\ \int_0^t \alpha(\theta)\,\nu(\theta,t)\mathrm{d}\theta \end{Bmatrix} \tag{2}$$

where N is the number of nuclei. The function $\nu(\theta, t)$ describes the volume of growing crystal, which is formed at θ time and is grown until t time. $\alpha(\theta)$ is characteristic for the formation rate of nuclei. If the growth rate is equal toward all dimension the $\nu(\theta, t)$ function can be expressed as:

$$\nu(\theta,t) = f_g\left(\int_0^t G(T)\mathrm{d}T\right)^d \tag{3}$$

where $G(T)$ is the growth rate at T temperature and f_g is a geometrical factor, which equals $4/3\pi$ in the case of spherical growth. The exponent d is the dimension of growth. Accordingly, crystallization process can be described in the case of three dimensional and spherulitic growth using Equation 4.

$$E(t) = kt^n = N\frac{4}{3}\pi(Gt)^3 \tag{4}$$

Based on equations 2-4 N can be calculated either for athermal or for thermal nucleation. If the number of nuclei is constant (athermal nucleation) and spherulitic three dimensional growth is supposed N can be expressed easily from Equation 4.

$$N = \frac{k}{\frac{4}{3}\pi G^3} \tag{5}$$

The situation is more difficult in the case of thermal nucleation, because the formation rate of the nuclei should be also included. The number of nuclei is changing during crystallization, thus it can be only calculated at a given crystallization time according to equation 6. However, this equation can be applied only until the development of the crystalline phase stops (practically under 95-97% of conversion), because it results in infinite number of nucleus at infinite time. If the final time (t_f) at high conversion of crystallization is used for calculation, equation 6 results in the number of nuclei at the end of crystallization.

$$N_f = \frac{kt_f}{\frac{4}{3}\pi G^3} = \left(Ae^{\left(-\frac{\Delta G_C^*}{kT}\right)}e^{\left(-\frac{Q^*}{RT}\right)}\right)t_f \tag{6}$$

where Q^* is the activation heat of the transport processes, which can be obtained from the WLF equation. ΔG_c^* is the free enthalpy of formation of a nuclei with critical size. The G can be measured at a discreet temperature using optical microscopy and k can be estimated from the evaluation of a crystallization curve recorded at the same temperature in a DSC. Usually the linearized form of Avrami equation (Equation 1) is used for evaluation of k and n.

$$\ln(-\ln(1-X)) = \ln(k) + n\ln(t) \tag{7}$$

X is the crystalline fraction at t time ($X=X_t/X_\infty$). The left side of Equation 7 have to be plotted against ln$t$ and n is the slope and k is the intercept of the straight line. Once the $G(T)$ and k data pairs are available N can be easily calculated. This proves clearly that theoretically the calculation of nucleus density is possible, but not easy. Moreover, the major drawback of these calculations is that $G(T)$ and k data can be obtained at isothermal conditions in a limited temperature range either in POM or in DSC. The temperature window of the two techniques is quite different thus the temperature range of such calculation is strongly limited. The crystallization becomes too slow at high temperatures, where the growth of the spherulites can be studied easily, but the crystallization curves recorded at these temperatures are too flat and their evaluation becomes unreliable. In spite of that the size of the spherulites becomes too small at low temperatures and thus the estimation of $G(T)$ is not possible, although the evaluation of crystallization isotherms recorded by DSC is easy at these temperatures. In order to solve this problem Lamberti et al. [20, 22] worked out an evaluation method for calculation of nucleus density from the DSC experiments only, moreover he summarized accurately the possibilities and limitations of these conventional equation in his recent work [22]. The method is based on the AKE equation as well. The method was developed for nucleated samples thus it supposes that athermal nucleation occurs. For the determination of N the $G(T)$ function should be known. They used the widely accepted Hoffmann-Lauritzen equation to describe the temperature dependency of growth rate.

$$G(T) = G_0 exp\left(-\frac{U^*}{R(T-T_g+T_\infty)}\right) exp\left(\frac{\kappa_G {T_m^0}^2 (T_m^0+T)}{2T^2(T_m^0-T)}\right) \quad (8)$$

where $G(T)$ is growth rate, R is the universal gas constant, ${T_m}^0$ is the equilibrium melting temperature of the polymer, T_g its glass transition temperature, T_∞ is a reference temperature used in William-Landel-Ferry equation, U^* the activation energy of transport processes, while G_0 and

κ_G are iterative parameters. The half time of crystallization can be modelled analogously to the growth rate using the following equation:

$$\frac{1}{t_{1/2}} = \frac{1}{t^0_{1/2}} exp\left(-\frac{U^*}{R(T-T_g+T_\infty)}\right) \exp\left(\frac{\kappa_t {T_m^0}^2 (T_m^0+T)}{2T^2(T_m^0-T)}\right) \quad (9)$$

where $t_{1/2}$ is the half time of crystallization. Using the equations above nucleus density can be expressed as:

$$N = \frac{3}{4\pi}\ln(2)\left(\frac{1/t_{1/2}}{G}\right)^3 = \left(\frac{3}{4\pi}\ln(2)\left(\frac{1/t^0_{1/2}}{G_0}\right)^3\right)\exp\left(-3\frac{(\kappa_t-\kappa_G){T_m^0}^2(T_m^0-T)}{2T^2(T_m^0-T)}\right) \quad (10)$$

The model of Lamberti el al. [20] was tested on nucleated and clarified samples during earlier studies [19] and we found that the nucleus density is a key parameter indeed from the point of view of optical properties. de Santis *et al*. [23] introduced a similar technique, which also capable to calculate nucleus density from isothermal crystallization curves. The crucial problem of the above mentioned calculation methods is that *N* can be obtained only from isothermal experiments, which is very time consuming experiments and the results of such calculation are difficult to be related to properties of product in practice. The characteristics of crystallization process under processing conditions were collected, studied and described in details by the research group of Janeschitz-Kriegl et al.[28, 29].

The kinetics of crystallization at constant cooling rates was described by Ozawa [30]. He modified the Avrami equation and introduced a new term, $\chi(T)$, which is the cooling function and contains both the nucleation and the growth. The formalism of this equation is very similar to that of Avrami equation except that $\chi(T)$ and the cooling rate (β) is written in the right side of Equation 7. The slope of the plotted line results in the Avrami constant and the slope is the $\chi(T)$ function, which contains the nucleation density as well. Unfortunately, the number of nuclei cannot be evaluated

directly from this simple equation. Only few attempts carried out to obtain nucleus density under non-isothermal conditions [31-33]. Boyer et al. [32] introduced recently an excellent work for description of crystallization at high cooling rates. The most important merit of this work is the unique technique for measurement of growth rate in wide temperature range at constant cooling rate. Unfortunately these works propose that the nucleation is instantaneous and athermal thus the number of nuclei is constant during the crystallization and can be obtained similarly to Equation 4. However, the reality is more complex and the change in the number of nuclei cannot be neglected according to our opinion. In addition all approaches concern this problem handles the growing spherulites as freely growing spheres, which is also a simplification of the reality. In fact spherulites grow freely only in the early stage of crystallization and later the spherulite boundaries meet and the development of the supermolecular unit stops. This statistical process is usually also neglected by the existing models. An excellent numerical approach was published by van Drongelen et al.[34], which makes possible to handle the complex crystallization process of iPP under non-isothermal conditions even under fast cooling rates.

Consequently, the aim of this work is to suggest a numerical calculation method based on the basic equations of crystallization kinetics for obtaining nucleus density from calorimetric crystallization curves recorded under non-isothermal conditions if the growth rate is known in wide temperature range. Nucleus density was calculated for nucleated and non-nucleated iPP homopolymer samples and the obtained N was correlated to the haze of injection molded samples in order to check the reliability of the results.

EXPERIMENTAL

Materials

TIPPLEN H3 iPP homopolymer, which is a neat reactor powder, was supplied by Tisza Chemical Group Ltd. was used as reference polymer (designed as H3). The MFR of the polymer was estimated according to ISO 1133 standard at 230 °C and 2.16 kg of load and it was between 8 and 15 dg min^{-1}. The polymer resin was stabilized using 2000 ppm of Irganox B215 (BASF Germany). Two types of heterogeneous nucleating agents (NA21E and NA71 supplied by Adeka-Palmarole, France) and one clarifier (Millad NX 8000, Milliken USA) were used for modification of crystalline structure. NA21E and NA71 were introduced in 500, 1000, 1500, 2000 and 3000 ppm and these nucleating agents were designed as N2 and N7 respectively. The clarifier (Millad NX 8000) is applied in larger concentrations (1000, 2000, 3000, 4000 and 5000 ppm) and it is designed as NX in the followings. The sample codes contain the code of the polymer, nucleating agent and its amount in ppm. For example H3-N2-500 means that 500 ppm of NA21E was introduced into H3 polymer.

The additives and the polymers were homogenized in two steps procedure. First the polymer power and the additives were homogenized in a Thyssen Henschel FM/A10 fluid type mixer at a rotation speed of 700 min^{-1} for 5 min. Subsequently, the homogenized powder was processed using a Brabender Plasti-Corder 42/7 twin screw extruder driven by a Brabender Plasti-Corder PLE 3000 driving unit. The temperature zones of the extruder were set to 210, 220, 230 and 230 °C and the rotation speed was 50 min^{-1}. 1 mm thick platelets were injection molded for haze measurements using a DEMAG IntElect electronic injection molding machine. The temperature zones of IM

machine were set to 200, 210, 220 and 230 °C and the temperature of the mold was 40 °C. The holding pressure was 700 and 400 bar during the injection and hold on stage respectively. The hold on time was 10 s.

Methods

Melting and crystallization characteristics of the polymers were studied using a Perkin Elmer DSC-7 calibrated by Indium and Tin reference materials. Samples between 3 and 5 mg were studied under pure Nitrogen atmosphere (20 mL min^{-1}). The thermal and mechanical prehistory of the samples was erased at 220 °C for 5 min. Subsequently, the samples were cooled to room temperature at different heating rates of 5, 10, 15 and 20 °C min^{-1}. The nucleus density was calculated from the crystallization curve recorded during cooling. Then the samples were heated up to 220 °C again at 10 °C min^{-1} in order to record the characteristic data of melting as well.

Thermooptical studies were carried out in order to determine the growth rate of the polymer at different temperatures. A Zeiss Axioscop was used for these studies. The samples were heated using a Mettler FP80 hot stage and the micrographs were captured using a Leica DMC 320 type digital camera and the evaluation of the images was performed by Leica IM50 software. The thermal and mechanical prehistory of the samples was eliminated at 220 °C for 5 min similarly to the DSC experiments. Then the samples were quenched to the crystallization temperatures and the growth of the spherulites was studied isothermally.

The optical properties (haze index) of injection molded platelets were measured using a Hunterlab ColorQuest XE apparatus according to the ASTM D1003D-95 standard.

THEORY OF CALCULATION

The kinetic equations (Equations 1-6) of crystallization describe the development of the crystalline phase as forming and growing of spheres in the materials. Unfortunately, the exact solution of the basic kinetic equations of crystallization can not be given under non-isothermal conditions because the overall rate constant (k) and the other constants refer to the transport processes in the polymer melt (Q^* and U^*) depend strongly on temperature. Consequently, the exact solution of this problem is very difficult if not impossible at all. However, the basic assumption of crystallization that the volume is filled up with continuously forming and growing spheres, can be applied for non-isothermal conditions as well and the development of crystalline volume can be directly calculated from the DSC curve. Consequently, the estimation of nucleus density is possible, but few assumptions should be considered for the calculations:

-The number of nuclei is changing during non-isothermal crystallization, thus rate of nucleation is changing continuously. In fact the overall rate is proportional to the supercooling ($k \sim \Delta T^{1.35}$)

-The growth rate of the polymer depends only on temperature and do not depend on nucleation.

-Crystallization takes place at large supercooling under dynamic conditions thus the entire process is in Growth Regime III and the Regime does not change.

-Crystallization is described by growing and forming of spheres, which are growing with the same rate toward all steric directions.

With respect to the assumptions above the first step of calculation is the determination of growth rate in wide temperature range by POM technique. Then the G_T function can be calculated by fitting Equation 8 to the experimental data and G_T function has to be simulated using the temperature range and increment applied during the cooling run in the DSC.

The second step is the calculation of the development of crystalline volume from the DSC curve directly.

$$V_{cr}^{t} = \frac{\Delta H_c^t \cdot m}{\Delta H_m^0 \cdot \rho_{cr}} = \frac{x_t \cdot m}{\rho_{cr}} \tag{11}$$

V_{cr}^{t} is the volume of crystalline fraction at *t* time or *T* temperature. We may note that the time and temperature points are equivalent using a constant cooling rate and every point of the DSC curve can be given as a function of time or temperature. ΔH_c^t is the partial crystallization enthalpy at *t* time, *m* is the sample mass, ΔH_m^0 is the equilibrium enthalpy of fusion [36] and its value is 148 Jg^{-1} for the α-modification of iPP. The ρ_{cr} is the density of crystalline fraction (0.936 gcm^{-3}) [37] and x_t is the conversion of crystallization.

Once the development of crystalline volume is known the V_{cr}^{t} function can be divided into infinitesimally small increments. In our case we used 1s as time increment (t_i), which corresponds to 0.17 °C at 10 °$Cmin^{-1}$ heating rate. The small increase in crystalline volume (ΔV_{cr}) in every incremental section can be calculated easily as:

$$\Delta V_{cr} = V_{cr}^{t} - \sum_{0}^{t-t_i} \Delta V_{cr} \tag{12}$$

We suppose that Equation 4 can be written to every small temperature increment and consequently *N* can be calculated in each small increment using the basic equations.

$$\Delta V_{cr} = N \frac{4}{3} \pi (G_T t_i)^3 \tag{13}$$

$$N = \frac{3\Delta V_{cr}}{4\pi (G_T t_i)^3} \tag{14}$$

G_T is the growth rate at a given temperature corresponding to the small increment investigated. The ΔV_{cr} however consists of two parts, because both the growth of existing nuclei and the formation of new nuclei have to be concerned. Thus ΔV_{cr} have to be written as:

$$\Delta V_{cr} = \sum_0^{t-t_i} \Delta v_{cr} + \Delta v_{cr}^t \tag{15}$$

The first part of Equation 16 ($\sum_0^{t-t_i} \Delta v_{cr}$) is the volume increase originated from the growth of all existing nuclei before *t* and the second part (Δv_{cr}^t) is the volume change due to the formation of new nuclei. The two parts can be expressed as:

$$\sum_0^{t-t_i} \Delta v_{cr} = \sum_0^{t-t_i} N \frac{4}{3} \pi (G_T t_i)^3 \tag{16}$$

$$\Delta v_{cr}^t = N_t \frac{4}{3} \pi (G_T t_i)^3 \tag{17}$$

Our goal is to calculate the number of new nuclei needed to obtain the measured increase of crystalline volume (N_t) in each small increment of crystallization, thus Δv_{cr}^t have to be expressed from Equation 15. Using Equations 16 and 17 the formula of N_t can be estimated as:

$$N_t = \frac{3\Delta V_{cr}}{4\pi (G_\tau t_i)^3} - \sum_0^{t-t_i} N \tag{18}$$

Unfortunately, Equation 18 can not be used for evaluation of nucleus density, because this mathematical formula describes the crystallization as the development of freely growing spheres. However, growing of spherulites is unhindered only in the early stage of crystallization and spherulites come into contact with each other during later stage of crystallization [38] leading to smaller number of growing spherulites than $\sum_0^{t-t_i} N$. We may suppose that the number of freely growing spherulites is somehow proportional to the conversion and it is large at the beginning and small at the end of crystallization. In order to consider this problem the sigmoidal equation of

random nucleation and subsequent growth of the original Avrami theory is incorporated into Equation 18. For simplicity let us define N_{t-t_i}, which equals to $\sum_0^{t-t_i} N$. In our case we supposed three dimensional growth and continuously changing nuclei number. Thus the number of active nuclei can be expressed as:

$$N_{t-t_i}\left(1-\left(4(1-x_t)\left(-ln(1-x_t)\right)^{3/4}\right)\right) \tag{19}$$

Using this correction function the number of subtracted spherulites can be modified during crystallization as a function of conversion (x_t). Equation 19 equals to N_{t-t_i} at x_t = 0 and it monotonously decreasing with increasing conversion. Accordingly, all growing spherulites are subtracted at the beginning of crystallization, which means that the change in crystalline volume originated from the formation of new nuclei mainly. After a short incubation time the number of subtracted nuclei decreases indicating that the growth of the existing supermolecular unit becomes more and more pronounced. However at larger conversion the number of freely growing spherulites decreases as a consequence of meeting of spherulite boundaries. According to equation 19 the number of subtracted existing spherulites increases again because the closed surfaces cannot contribute to the development of crystalline phase. Although, we have to note here that the correction presented in this work may not consider all statistical effects during crystallization the development of a more sophisticated internal function might open a further discussion in the future:

$$N_t = \frac{3\Delta V_{cr}}{4\pi(G_\tau t_i)^3} - N_{t-t_i}\left(1-\left(4(1-x_t)\left(-ln(1-x_t)\right)^{3/4}\right)\right) \tag{20}$$

$$N = \sum_0^{t_f} N_t \tag{21}$$

The value of ΔV_{cr} is derived from the crystallization curve directly, G_T is simulated value for the entire process. The sum of N_t until the end of crystallization (t_f) results in the nucleus density at a constant cooling rate.

RESULTS AND DISCUSSION

Melting and crystallization characteristic of nucleated samples

As it was described in the Materials section our concept was tested on nucleated iPP homopolymer samples. The characteristic data of crystallization and melting was evaluated from the cooling and heating runs respectively after elimination of thermal and mechanical prehistory of the samples (Table 1).

Table 1 The characteristic data of melting and crystallization

Sample code	**Cooling run**				**Second heating run**		
	T_{cp} /°C	T_{cf} /°C	T_{c0} /°C	ΔH_c /Jg^{-1}	T_{mp} /°C	T_m /°C	ΔH_f /Jg^{-1}
H3-ref	112.6	108.4	117.6	-97.2	164.0	173.1	94.6
H3-N2-500	125.3	121.6	128.7	-98.6	167.4	170.9	101.4
H3-N2-1000	126.8	123.6	129.9	-98.7	166.7	169.8	104.8
H3-N2-1500	127.1	124.0	130.2	-98.2	166.5	169.6	104.7
H3-N2-2000	127.3	124.0	130.6	-100.4	166.7	170.0	105.5
H3-N2-3000	128.3	124.5	131.6	-99.0	167.2	171.0	103.8
H3-N7-500	125.8	122.1	129.4	-101.1	166.9	170.7	103.8

H3-N7-1000	127.0	122.9	130.6	-102.2	166.9	171.1	104.0
H3-N7-1500	128.0	124.3	131.4	-103.5	166.9	170.5	104.2
H3-N7-2000	128.8	125.4	132.4	-103.0	167.0	169.9	101.7
H3-N7-3000	129.8	126.7	132.9	-102.8	165.9	169.3	102.5
H3-NX-1000	113.6	110.6	116.1	-96.0	162.9	169.0	97.2
H3-NX-2000	125.0	121.9	126.8	-100.4	166.2	169.8	106.0
H3-NX-3000	128.8	123.9	133.9	-101.9	167.2	170.9	110.5
H3-NX-4000	130.5	126.6	133.7	-102.7	166.9	170.9	110.1
H3-NX-5000	131.1	127.5	134.3	-101.9	166.5	170.2	110.2

The onset (T_{c0}), peak (T_{cp}) and end (T_{cf}) temperature of crystallization as well and the enthalpy of crystallization (ΔH_c) were evaluated from the crystallization curve. The peak (T_{mp}) and end (T_m) temperature as well as the enthalpy of fusion (ΔH_f) were obtained from the melting curves recorded during second heating. The presented data indicate clearly that the nucleating agents are efficient and their efficiency is characterized by the shift of T_{cp} and the change in crystallinity (Figure 1.)

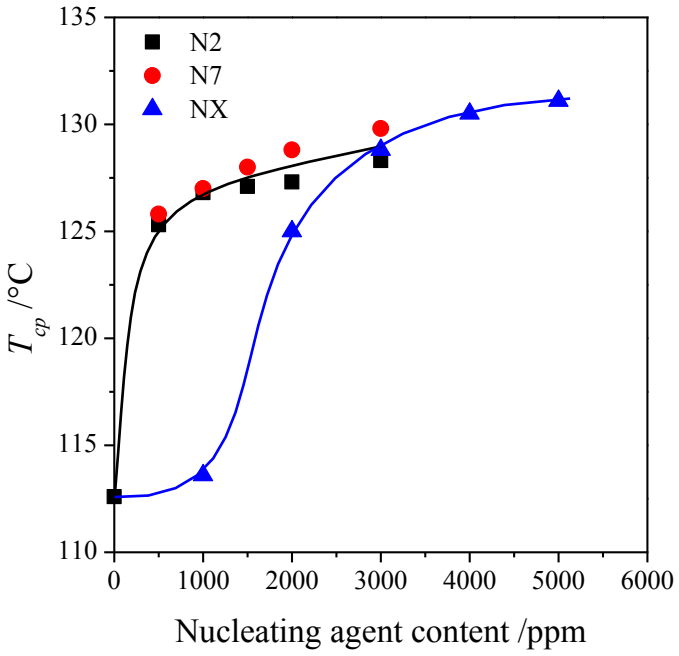

Figure 1 The efficiency of selected nucleating agents in iPP

It can be clearly seen that NX is the most effective additive, because T_{cp} is the highest in the presence of this clarifier. The efficiency N2 and N7 is similar, but smaller compared to that of NX. However, we have to point out that NX is soluble in iPP melt thus it is effective only at relative large content [8-10, 14, 16, 17]. N2 and N7 are not soluble nucleating agents, thus they are effective even at low concentrations. The considerable change in T_{cp}, indicates that considerable increase in nucleus density might be expected in the studied samples due to the efficiency of the nucleating agents used.

Calculation of nucleus density

As it was described before the first step of calculation of N is the determination of G_T function. The growth rate of spherulites was derived from POM micrographs taken during crystallization under isothermal crystallization at different temperatures (T_c). The size of five spherulites was measured during crystallization and an example is demonstrated in Figure 2.

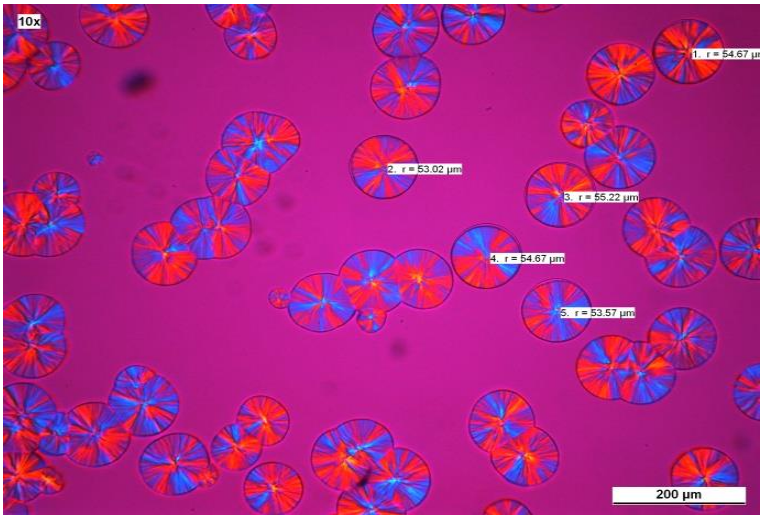

Figure 2 The spherulitic structure of H3 iPP crystallized at 132 °C for 14 min

The radius of spherulites was plotted against time for all the spherulites. The growth rate of the spherulites is linear at isothermal temperature thus the plotted data describes a straight line and the slope of this line is the linear growth rate ($G(T)$) at T_c (Figure 3). The data points fit nicely to a straight line ($R > 0.99$). Similar diagrams were obtained at 134, 136, 138, 140 and 142 °C and the $G(T)$ was calculated for all these temperatures. After all $G(T)$ data were obtained Equation 8 is fitted to these data. The value of constants used during the fitting procedure appears in Table 2. We have used the same constants as it had been used before in order to make the present results comparable with the previous ones [19, 20].

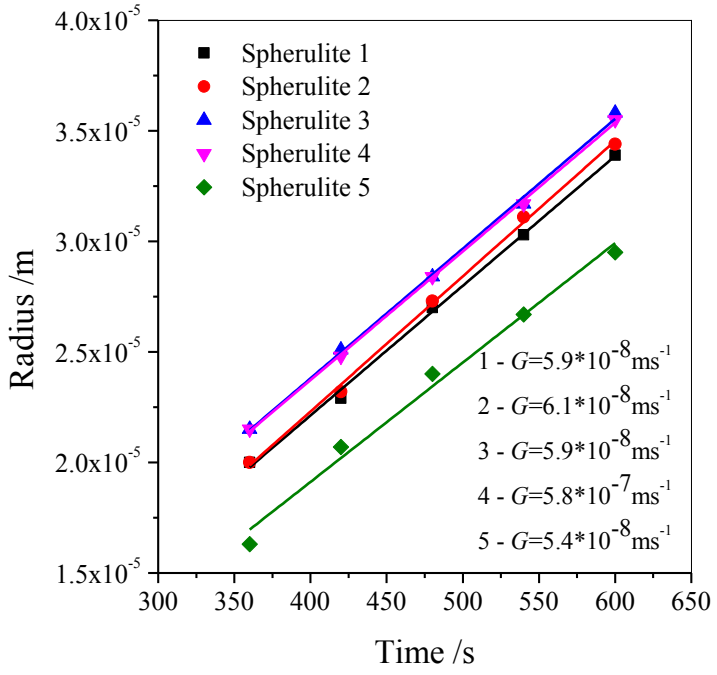

Figure 3 The growth of spherulites in H3 iPP at 132 °C

Table 2 The value of constants used during fitting of Equation 8 to the measured G_T data

Constant /dimension	Value	Reference
T_g /K	263.15	[39]
T_m^0 /K	481.15	[36]
T_∞ /K	30.0	[20]
$\frac{U^*}{R}$ /K	755	[20]
κ_G	fitted	
G_0 /ms^{-1}	fitted	

The fitted curve is presented in Figure 4. The most difficult point of this calculation method is the determination of G_T function, because $G(T)$ data can be measured experimentally only in narrow

temperature range using conventional hot stage microscopy. Although, Ratajski et al.[40] developed a unique technique for measurement of $G(T)$ in wide temperature range. They could estimate the growth rate of a transcrystalline layer in wide temperature range indeed, however this technique requires special instrumentation thus it is not available in most laboratories. In order to demonstrate the reliability of the calculation the crystallization curve is also included into Figure 4. It is clearly visible that the crystallization of the polymer takes place near to the experimental data. Moreover, efficient nucleation shifts the crystallization peak toward higher temperatures, thus the crystallization of nucleated samples will be even closer to the experimentally measured G_T data. The simulated G_T function was compared to literature data obtained by Gahleitner et al.[41] using the unique technique mentioned above (see the black squares in Figure 4). It can be established that the simulated and experimentally obtained data are in the same order of magnitude. In addition our simulated data are similar to those simulated by van Drongelen et al.[34]. The matching of G_T data is reasonably good close to the temperature range of crystallization process of the polymer at relatively slow cooling rate used in this study. As a consequence we may suppose that despite of the narrow temperature window of POM experiments the simulated G_T data are reliable in the temperature range of crystallization and can be used for the calculation of N.

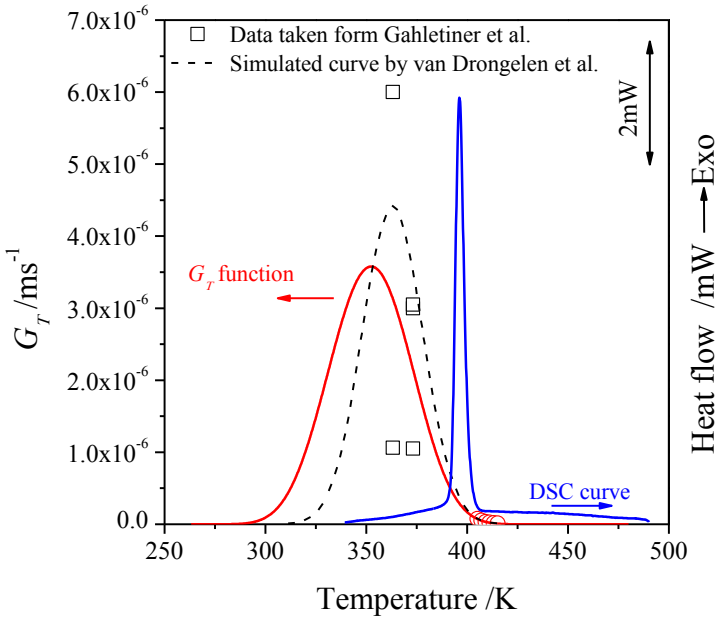

Figure 4 The simulated growth rate function (G_T) and the crystallization curve recorded by DSC at 10 °Cmin^{-1} of cooling rate (Literature data was taken from[34, 41])

Once the simulated G_T function and the conversion curve (x_t) of crystallization (simply the integrated crystallization curve) are estimated in the same temperature range, the calculation of nucleus density is possible. The development of crystalline volume (V_{cr}^t) can be calculated according Equation 12 and is plotted in Figure 5. During the calculation of N, this V_{cr}^t function is divided into infinitesimally small sections, wherein the temperature (T_i) and time (t_i) were 0.17 °C and 1 s respectively. ΔV_{cr} can be calculated from Figure 5 in every small increments using Equation 14.

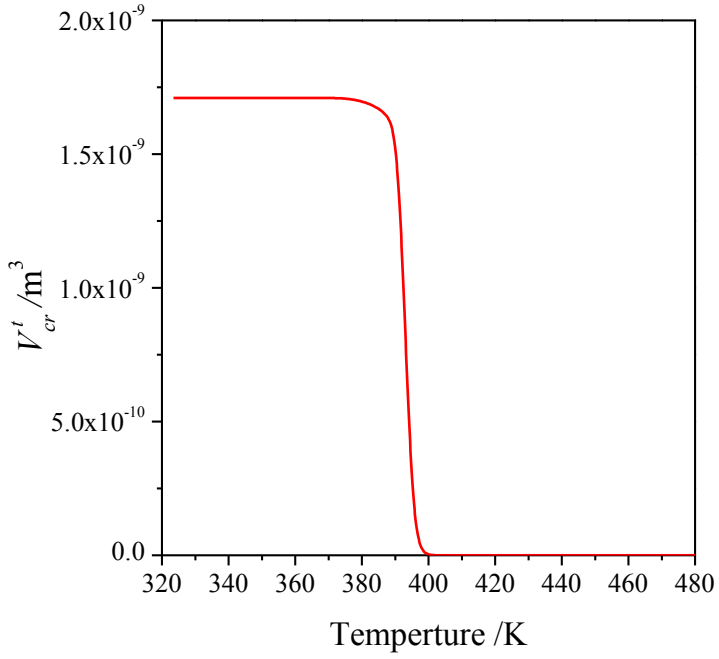

Figure 5 Development of crystalline volume in H3 iPP at cooling rate of 10 °Cmin^{-1}

After calculation of ΔV_{cr} the nucleus density can be calculated using the G_T at the temperature where the increment is and t_i according to Equations 20 and 21. The calculated N function is presented in Figure 6. It can be clearly seen that the nucleus density increases steeply the early stage of crystallization. The rate of nucleus formation becomes the fastest also in the early stage of crystallization, where the increase of crystallization rate is the steepest, which is in good agreement of the general theories of crystallization kinetics. Subsequently, the rate of nucleus formation slows down at larger conversions because of the kinetic hindering and the small volume of free melt, wherein nucleation can occur. The value of N is the sum of N_i values in the entire conversion range (see Equation 21) and gives the final number of nucleus in the sample formed during crystallization.

Since the relative error of the experimental data is very large at the beginning of crystallization the N_t curve should be summarized in the conversion range of $0.003 < x_t < 1$ in order to get reliable

result. The estimated nucleus density is $8.95*10^8$ m^{-3} in the case of non-nucleated H3 iPP. The N_t function can be plotted either against temperature or against time because of the constant cooling rate.

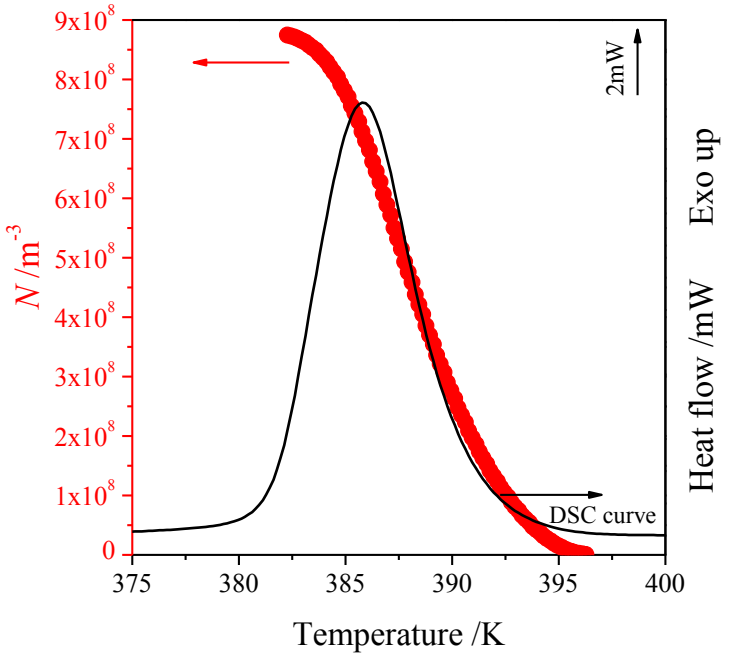

Figure 6 The N_t function together with the crystallization curve of H3 iPP crystallized at 10 °Cmin^{-1} of cooling rate

It was supposed that the growth rate depends only on temperature, thus the G_T function have to be determined only for the non-nucleated polymer and the estimated G_T function can be used for the calculation of N of the nucleated samples as well. This assumption is in good agreement with the basic theory of crystallization, because the growth of crystalline front occurs via secondary nucleation [35]. That means that the crystalline phase covers the heterogeneous surface at the initial stage of crystallization and the secondary nuclei form on the surface of the polymer instead of the nucleating agent. The effect of nucleating agents on nucleus density is demonstrated in Figure 7.

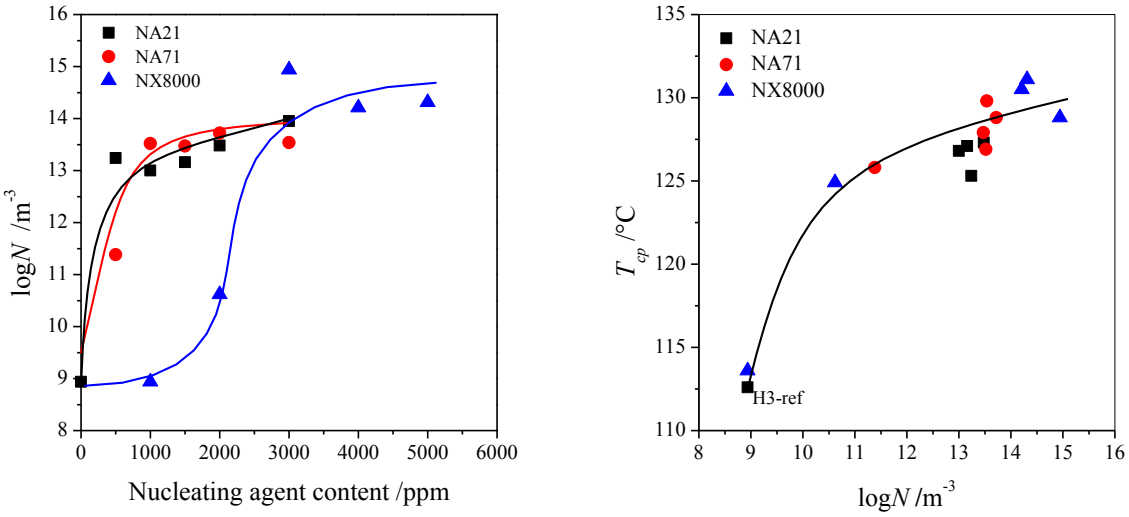

Figure 7 The effect of nucleating agent on the nucleus density (a) and the correlation between T_{cp} and N_t (b)

The results presented in Figure 7a indicate that N increases more than five orders of magnitude, which is according to our expectations. Moreover, it is clearly observable in Figure 7b that N correlates also with T_{cp}. In other words, the more efficient is a nucleating agent, the larger is the nucleus density in its presence. However we have to note that the deviation of the data points from the general trend hints that the nucleus density depends not only on nucleation activity. In addition we have to note that the obtained N values in the presence of efficient nucleating agents are in the order of 10^{14} m^{-3}, which are close to the nucleus density values obtained by other research groups [34, 41].

The effect of nucleus density has been correlated to the optical properties thus we can check the reliability of our results by plotting haze (H) as s function of N (Figure 8). A clear correlation can be established between N and H and the results indicate unambiguously that optical properties improve only above a critical N, because the size of spherulites becomes so small at this N value that they do not interfere with the visible light anymore. The results explain the strong correlation

between H and T_{cp} as well [42, 43], which correlation is used frequently by the industrial practice. However, we have to call the attention to the fact that this correlation is not necessarily valid in every case. If the concentration of a highly active nucleating agent is small the nucleus density will be proportionally smaller leading to slightly improved optical properties only[19]. Calculation of nucleus density is essential in every case, when the optical properties of a semicrystalline polymer are investigated, because the explanation of improved optical properties is the change in supermolecular structure.

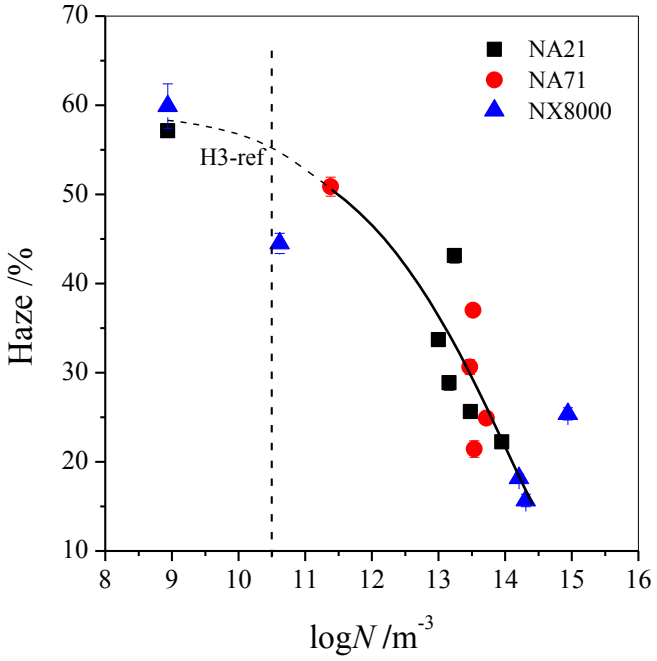

Figure 8 The effect of change in nucleus density on the optical properties

The effect of cooling rate on the nucleus density

Using our calculation model, nucleus density of polymers can be reliably calculated from DSC curve recorded at constant heating rate. However, it is well-known that the nucleus density depends on the cooling rate as well. According to literature sources, nucleus density increases with increasing cooling rate [35, 44, 45]. The explanation is also well-known that the crystallization process shifts toward the lower temperatures at faster cooling and the rate of nucleus formation increases also at larger supercooling leading to larger nucleus density. Therefore we checked how our model handles the effect of cooling rate. Non-nucleated H3 polymer was cooled to room temperature at 5, 10, 15 and 20 °Cmin^{-1} and the nucleus density was calculated from each cooling curve. There are two possibilities to calculate nucleus density at different heating rates, because either T_i or t_i can be constant, but both of them cannot be kept constant at the same time. If T_i is constant the faster cooling results in shorter t_i and vice versa. Similarly to that the faster or slower cooling rates results in smaller and larger T_i in the case of constant t_i. Nucleus density was calculated according to both ways with constant T_i or t_i as well. The results are depicted in Figure 9.

The results indicate clearly, that T_i must be kept constant during the calculation and fixing of t_i results in misleading results. The results are easy to be explained because at constant t_i the temperature window increases and decreases with changing the cooling rate. However, we have to call the attention that the temperature window of the calculation procedure must be small enough to use Equation 4 with constant G_T. In the case of larger cooling rate the temperature increment will be too large and the Equation 4 cannot be used with constant G_T. Using constant T_i the results are in good agreement with the basic phenomenon of crystallization, because N should increase with increasing of cooling rate. Consequently, using the calculation method proposed in this work the T_i must be kept constant if the effect of cooling rate is studied. We have to remark here that the proposed approach is valid only in the case of limited cooling rates, because at very high cooling

rates the formation of nuclei is suppressed also, which can be seen in the work of Boyer et al. [32] or van Drongelen et al. [34]. In addition the proposed model could not be tested also in the case if crystallization takes place in the vicinity of glass transition temperature (T_g), because it requires special fast scan calorimetry to perform such experiments [46]. Accordingly, the extension of this calculation approach to extreme fast cooling rates could be the direction of further studies.

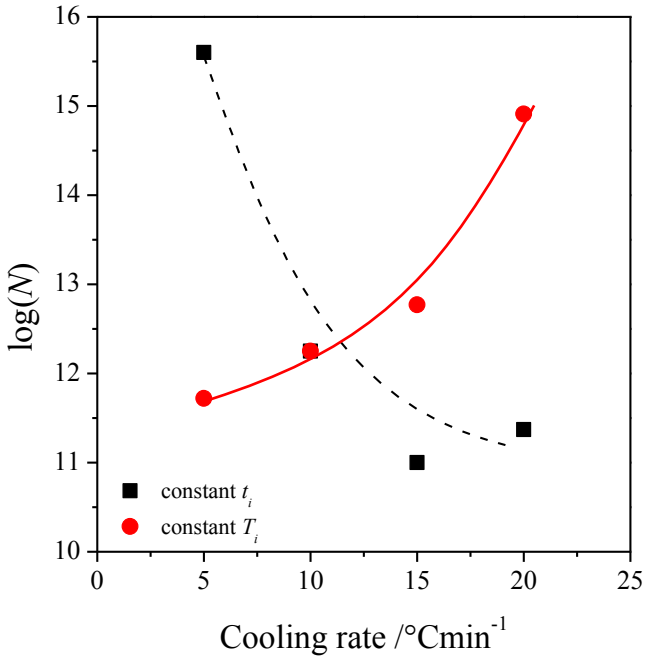

Figure 9 Effect of cooling rate on nucleus density calculated with constant T_i and t_i

CONCLUSIONS

A new approach was proposed in this work for calculation nucleus density from crystallization curve recorded under non-isothermal condition at constant cooling rate. The calculation approach

was tested on iPP homopolymer samples with and without efficient nucleating agent. The obtained results proved that the nucleus density increases more than five orders of magnitude in the presence of efficient nucleating agent. These results are in good agreement with earlier nucleus density data obtained by different approaches as well as with our expectations and indicate clearly that the new approach results in reliable nucleus density values. Our approach was tested in the non-nucleated polymer at different cooling rates and it was found that if the temperature increment is fixed during the calculation then it is capable to calculate the nucleus density at different cooling rates.

The calculated nucleus density values were correlated to the optical properties of injection molded samples and it was demonstrated unambiguously that the haze of the polymer decreases above a critical nucleus density. Moreover, the results revealed also that the nucleus density in the presence of a sorbitol based clarifier is much larger compared to that of a conventional nucleating agent leading to much better optical properties.

ACKNOWLEDGEMENTS

The Authors would like to express their gratitude to the János Bolyai Research Scholarship of the Hungarian Academy of Sciences and for the financial support of the National Scientific Research Fund of Hungary (OTKA Grant PD 109346) for the project on the structure-property correlations of polymeric materials.

REFERENCES

1. Moore, E. P., *Polypropylene Handbook: Polymerization, Characterization, Properties, Processing, Applications*. Hanser-Gardner Publications: Cincinnati, 1996; p 1-419.
2. Meeten, G. H., *Optical Properties of Polymers*. Elsevier: London & New York, 1986; p 1-398.
3. Haudin, J. M., Optical Studies of Polymer Morphology. In *Optical Properties of Polymers*, Meeten, G. H., Ed. Elsevier: London, 1986; pp 167-264.
4. Binsbergen, F. L. *Polymer* **1970,** 11, (5), 253-267.
5. Varga, J., Crystallization, Melting and Supermolecular Structure of Isotactic Polypropylene. In *Polypropylene: Structure, Blends and Composites*, Karger-Kocsis, J., Ed. Chapmann&Hall: London, 1995; Vol. 1, pp 56-115.
6. Kotek, J.; Kelnar, I.; Baldrian, J.; Raab, M. *Eur. Polym. J.* **2004,** 40, (4), 679-684.
7. Gahleitner, M.; Grein, C.; Kheirandish, S.; Wolfschwenger, J. *Int. Polym. Proc.* **2011,** 26, (1), 2-20.
8. Marco, C.; Ellis, G.; Gomez, M. A.; Arribas, J. M. *J. Appl. Polym. Sci.* **2002,** 84, (13), 2440-2450.
9. Kristiansen, M.; Werner, M.; Tervoort, T.; Smith, P.; Blomenhofer, M.; Schmidt, H. W. *Macromolecules* **2003,** 36, (14), 5150-5156.
10. Kristiansen, M.; Tervoort, T.; Smith, P. *Polymer* **2003,** 44, (19), 5885-5891.
11. Kristiansen, P. M.; Gress, A.; Smith, P.; Hanft, D.; Schmidt, H. W. *Polymer* **2006,** 47, (1), 249-253.
12. Mohmeyer, N.; Schmidt, H. W.; Kristiansen, P. M.; Altstadt, V. *Macromolecules* **2006,** 39, (17), 5760-5767.
13. Thierry, A.; Straupe, C.; Wittmann, J. C.; Lotz, B. *Macromolecular Symposia* **2006,** 241, 103-110.
14. Lipp, J.; Shuster, M.; Terry, A. E.; Cohen, Y. *Langmuir* **2006,** 22, (14), 6398-6402.
15. Jin, Y.; Hiltner, A.; Baer, E. *J. Polym. Sci. Pt. B-Polym. Phys.* **2007,** 45, (14), 1788-1797.
16. Balzano, L.; Rastogi, S.; Peters, G. W. M. *Macromolecules* **2008,** 41, (2), 399-408.
17. Zhang, Y. F.; Li, X.; Wei, X. S. *J. Therm. Anal. Calorim.* **2010,** 100, (2), 661-665.
18. Liu, T.; Meng, H.; Sheng, X. Y.; Zhang, X. *Polymer - Plastics Technology and Engineering* **2011,** 50, (11), 1165-1169.
19. Menyhárd, A.; Gahleitner, M.; Varga, J.; Bernreitner, K.; Jääskeläinen, P.; Øysæd, H.; Pukánszky, B. *Eur. Polym. J.* **2009,** 45, (11), 3138-3148.
20. Lamberti, G. *Polym. Bull.* **2004,** 52, (6), 443-449.
21. Ma, Z.; Steenbakkers, R. J. A.; Giboz, J.; Peters, G. W. M. *Rheologica Acta* **2011,** 50, (11-12), 909-915.
22. Lamberti, G. *Eur. Polym. J.* **2011,** 47, (5), 1097-1112.
23. Santis, F.; Pantani, R. *J. Therm. Anal. Calorim.* **2013,** 112, (3), 1481-1488.
24. Mubarak, Y.; Harkin-Jones, E. M. A.; Martin, P. J.; Ahmad, M.; Spe, *Crystallization of Isotactic Polypropylene: Comparison Between Alpha and Beta Growth Rates*. 2000; p 1626-1630.
25. Chen, J. H.; Chang, Y. L. *J. Appl. Polym. Sci.* **2007,** 103, (2), 1093-1104.
26. Avrami, M. *J. Chem. Phys.* **1940,** 8, 212.
27. Avrami, M. *J. Chem. Phys.* **1939,** 7, 1103.

28. Janeschitz-Kriegl, H. *Colloid Polym. Sci.* **2003,** 281, (12), 1157-1171.
29. Liedauer, S.; Eder, G.; Janeschitzkriegl, H.; Jerschow, P.; Geymayer, W.; Ingolic, E. *Int. Polym. Proc.* **1993,** 8, (3), 236-244.
30. Ozawa, T. *Polymer* **1971,** 12, 150-158.
31. Martinelli, A.; Cali, M.; D'Ilario, L.; Francolini, I.; Piozzi, A. *J. Appl. Polym. Sci.* **2012,** 123, (5), 2697-2705.
32. Boyer, S. A. E.; Robinson, P.; Ganet, P.; Melis, J. P.; Haudin, J. M. *J. Appl. Polym. Sci.* **2012,** 125, (6), 4219-4232.
33. Devisme, S.; Haudin, J. M.; Agassan, J. F.; Rauline, D.; Chopinez, F. *Int. Polym. Proc.* **2007,** 22, (1), 90-104.
34. van Drongelen, M.; van Erp, T. B.; Peters, G. W. M. *Polymer* **2012,** 53, (21), 4758-4769.
35. Wunderlich, B., *Crystal Nucleation, Growth, Annealing*. Academic Press: London, 1979; Vol. 2, p 1-461.
36. Monasse, B.; Haudin, J. M. *Colloid Polym. Sci.* **1985,** 263, (10), 822-831.
37. Clark, E. J.; Hoffman, J. D. *Macromolecules* **1984,** 17, (4), 878-885.
38. Varga, J. *J. Mater. Sci.* **1992,** 27, (10), 2557-2579.
39. Phillips, P., J.; Mezghani, K., Polypropylene, Isotactic (Polymorphism). In *The Polymeric Materials Encyclopedy,* Salamon, J., C., Ed. CRC Press: Boca Raton. FL, 1996; Vol. 9, pp 6637-6649.
40. Ratajski, E.; JaneschitzKriegl, H. *Colloid Polym. Sci.* **1996,** 274, (10), 938-951.
41. Gahleitner, M.; Bachner, C.; Ratajski, E.; Rohaczek, G.; Neissl, W. *J. Appl. Polym. Sci.* **1999,** 73, (12), 2507-2515.
42. Horváth, Z.; Menyhárd, A.; Doshev, P.; Gahleitner, M.; Vörös, G.; Varga, J.; Pukánszky, B. *ACS Applied Materials & Interfaces* **2014,** 6, (10), 7456-7463.
43. Horváth, Z.; Gyarmati, B.; Menyhárd, A.; Doshev, P.; Gahleitner, M.; Varga, J.; Pukánszky, B. *RSC Advances* **2014,** 4, (38), 19737-19745.
44. Wunderlich, B. *J. Therm. Anal. Calorim.* **2007,** 89, (2), 321-356.
45. Wunderlich, B., *Thermal Analysis of Polymeric Materials*. Springer: Berlin, 2005; p 894.
46. De Santis, F.; Adamovsky, S.; Titomanlio, G.; Schick, C. *Macromolecules* **2006,** 39, (7), 2562-2567.

TABLE OF CONTENT GRAPHIC

Determination of nucleus density in semicrystalline polymers from non-isothermal crystallization curves

Alfréd Menyhárd, Márton Bredács, Gergely Simon, Zsuzsanna Horváth